

# MODELING AND NUMERICAL SIMULATION OF TURBULENT PREMIXED FLAMES IMPINGING ONTO A WALL

Ahmed Neche\*, Zineddine Youbi, Rachid Renane

Laboratory of aeronautical sciences, aInstitute of Aeronautics and Space Studies, University of Blida1  
Bp 270, Route de Souma 09000 Blida, Algeria

**Abstract:** This paper will present an algebraic model closure of the turbulent fluxes as the sum of two contributions acting in opposite directions, one induced by turbulent motions and the other by thermal expansion. The turbulent transport is analyzed that for a sufficiently high turbulence level, the flame is unable to impose its own dynamics to the flow field, and the turbulent transport is of the gradient transport type for the reacting scalar  $c$  and when the turbulence level remains low, the thermal expansion due to heat release dominates the process of turbulent scalar transport and the turbulent transport is of a counter gradient turbulent transport.

. The combustion will occur in a variable equivalence ratio and as partially premixed combustion is highlighted as one of the most relevant and important modeling challenges in the field of turbulent premixed combustion, we will use the LW-P model of combustion for this situation. The resulting model is combined with the second order model of turbulence  $R_{ij}, \epsilon$  has evidenced the pressure drop across the flame due to counter gradient diffusion turbulent fluxes which has well predicted the jump of the axial velocity across the flame brush. A numerical simulation which corresponds to the experimental conditions of the experiment of Escudié and Haddar is presented in order to validate the model. The comparison of the results with the measurements were showing remarkable consistency and indicates that the model is a valid approach for predicting partially turbulent premixed flames stabilized in a stagnation flow.

**Key words:** Partially premixed combustion, Stagnating flow, Libby-Williams-Poitiers model, Numerical combustion simulation, Counter gradient diffusion turbulent fluxes

## 1. Introduction

Reacting turbulent flows present problems of important economic consequence in many fields of science. Premixed turbulent flames are of increasing practical importance and remain a significant research challenge in the combustion community. These flames represent a key element in the implementation of low emissions burners for a variety of industrial applications [1].

Turbulent premixed combustion is a highly complex process characterized by several phenomena and it is crucial for the researchers to understand the complexities of combustion to increase the efficiency of combustion systems.

The problems are made difficult because of the fact that the rates of reaction of concern are highly non linear functions of temperature and species concentrations. The turbulence in the flow engenders mixing of non uniformities in species and temperature and the rates of this mixing are usually not fast compared with the rates of reaction. As a consequence, large spatial and temporal fluctuations occur in the scalar quantities (composition, temperature ...) [2].

The crucial influence of thermal expansion phenomena upon the large scale features of turbulent premixed reactive flows was foreseen more than 50 years ago by Karlovitz et al. Flame generated turbulence, whose existence was theoretically confirmed by the later work of Libby and Bray is merely considered as a hypothesis able to explain the experimental measurements. The associated

---

\* **Corresponding author:** Rachid Renane  
E-mail: r.renane@yahoo.fr

phenomena, namely production of turbulence by the flame, and counter gradient diffusion were then evidenced experimentally [3].

The scientists undertake the fundamental research and the insights from research in combustion fundamentals are transferred to the industry. In fact, this approach is handled with model developments, implementation of models in numerical simulations and validation of the numerical results with experimental measurements.

A complete model of premixed turbulent combustion must take into account the mutual interaction of turbulence, chemistry reactions and fluid flow. The model is a simplified way of describing and predicting the physical phenomena.

The development of accurate and efficient models for turbulent premixed combustion is one of the most challenging tasks facing the combustion community today [4].

When simulating combustion of a turbulent gas mixture, characterized by large magnitude of temperature fluctuations, the key challenge consist of averaging quantities that depend non linearly on the temperature. To resolve the problem, fresh reactants and equilibrium combustion products are often assumed to be separated by thin, inherently laminar, self propagating layers called flamelets that are wrinkled and stretched by turbulent eddies [5-8].

Many laboratories have extensively studied experimentally turbulent premixed combustion in stagnating flows impinging on a wall [9-14]. The advantage of this geometry is the statistically planar flame brush shape which permits the governing equations to be reduced to similarity [9]. In these last years, many numerical and experimental investigations have been devoted to turbulent premixed reactive flow impinging on a flat plate. [12-17].

In modeling turbulent premixed combustion with the assumption of single step chemistry, the mass fractions of the reactive species are expressed in term of a single reduced mass fraction: the reaction progress variable  $c$ .

The progress variable ranges from zero in fresh gases to unity in burnt gases. The term of turbulent flux  $\overline{\rho u_i'' c''}$  in the transport equation for the mean reaction progress variable  $\tilde{c}$  was usually closed by simple classical gradient eddy –viscosity model:

$$\overline{\rho u_i'' c''} = -\frac{\mu_t}{\sigma} \frac{\partial \tilde{c}}{\partial x_i} \quad (1)$$

Theoretical and experimental works (Clavin and Williams [18] ), (Libby and Bray [19]), (Kalt et al [20]), have shown that this assumption may be wrong in some premixed turbulent flames and counter gradient turbulent transport may be observed.

Veynante et al [21] have analyzed the occurrence of counter gradient turbulent transport using direct numerical simulation (DNS) and the results demonstrate the power of DNS to help in the modeling of turbulent combustion.

The counter gradient diffusion phenomenon can be explained by the work of Libby and Bray [19] which was focused on the turbulent transport term  $\overline{\rho u_i'' c''}$ .

The flame was analyzed as flamelet separating fresh reactants ( $c=0$ ) and burnt products ( $c=1$ ) and the turbulent flux is expressed as:

$$\overline{\rho u_i'' c''} = \tilde{\rho} \tilde{c} (1 - \tilde{c}) (\tilde{u}_i^b - \tilde{u}_i^a) \quad (2)$$

The expressions (1) and (2) may describe opposite fluxes: consider a left travelling one dimensional turbulent flame, because of thermal expansion the conditional velocity in the burnt gases,  $\tilde{u}_i^b$ , is expected to be larger than the conditional velocity in the fresh gases,  $\tilde{u}_i^a$ .

According to equation (2) the turbulent flux,  $\overline{\rho u_i'' c''}$ , is expected to be positive. On the other hand, as the mean progress variable gradient is also positive, equation (1) leads to a negative value of  $\overline{\rho u_i'' c''}$ . This situation is

known as counter gradient turbulent transport or counter gradient turbulent diffusion and it is a key point of the BML (Bray-Moss-Libby) analysis.

This paper will present the case of combustion of lean mixtures taking into account the dilution of fresh reactants and burnt products by the surrounding air. The combustion will occur in a variable equivalence ratio and as partially premixed combustion is highlighted as one of the most relevant and important modeling challenges in the field of turbulent premixed combustion [22], we will use the Libby-Williams-Poitiers (LW-P) model of combustion for this situation [23]. This model is the generalization of the Libby-Williams (LW) model [24] by introducing a multi-Dirac probability density functions (Pdf). The modeling of partially premixed flames requires the use of two independent scalar variables so; we will use the mixture fraction and the fuel mass fraction for the progress of chemical reactions. The combustion model is combined with the second order model of turbulence  $R_{ij} - \varepsilon$  in order to well predict the main structure of the flame zone in the case of stagnating turbulent flames [14,15].

When a new model is proposed to be used, the choice of the first test problem for assessing the model is of paramount importance in order to understand whether or not the model deserves further study [25].

In order to satisfy the above criteria, the problem of countergradient scalar transport in impinging jet flames is chosen to validate our model since the direction of the turbulent flux is controlled by the conditioned velocities in one hand and there were performed some experimental investigations of counter gradient scalar transport by several research groups in the other hand for these flames. A numerical simulation is carried out in order to validate the resulting model and the computational results are compared with the experimental measurements done by Escudié and Haddar [10] where that flame is associated with the

flamelet regime of premixed turbulent combustion addressed by the model.

## 2. Experimental Setup

The schematic of the burner for the stagnation flow stabilized flame configuration is shown in figure 1.

We will be referred to the conditions of the experimental study of D. ESCUDIE and E. HADDAR [10] where the diameter of the inner fuel-air jet  $D$  is 66 mm and the stagnation flow is generated by placing a circular stagnation plate of a diameter of 400 mm at a distance  $H$  equal to 66mm above the exit jet.

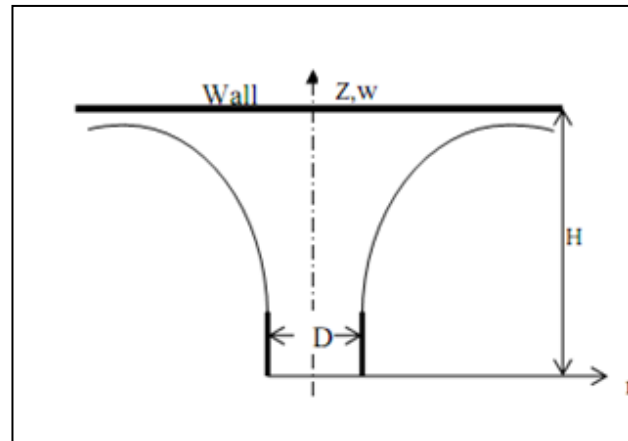
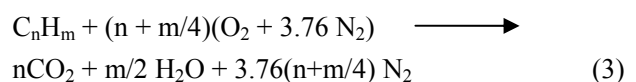


Fig.1 Burner geometry

The reactants are a mixture of  $CH_4$  and Air at an equivalence ratio  $\Phi$  equal to 0.9. The velocity at the exit of the burner is uniform and equal to 4m/s. The turbulence intensity and the integral length scale are of 9% and 1 mm respectively. [10]

## 3. Formulation of the thermochemistry

The Libby-Williams (LW) model [23], [24], [26], [27] for partially premixed turbulent flames represents the combustion of hydrocarbon air mixture through a global chemical reaction [22]:



Denoting  $Y_i$  ( $i= 1, \dots, 5$ ) the mass fractions of species  $O_2$ ,  $C_nH_m$ ,  $H_2O$ ,  $CO_2$  and  $N_2$ , respectively, and  $Z_j$  ( $j=1, \dots, 3$ ) the mass fractions of elements  $O_2$ ,  $H_2$  and  $C$ , respectively, the following balance equations are written as:

$$\begin{aligned} Z_1 &= Y_1 + \mu_{13} Y_3 + \mu_{14} Y_4 \\ Z_2 &= \mu_{22} Y_2 + \mu_{23} Y_3 \\ Z_3 &= \mu_{32} Y_2 + \mu_{34} Y_4 \\ Y_5 &= 1 - Z_1 - Z_2 - Z_3 \end{aligned} \quad (4)$$

with  $\mu_{ij} = m_i/W_j$ , where  $m_i$  is the mass of element  $i$  in species  $j$ , and  $W_j$  is the molar weight of species  $j$ .

For the fresh mixture, the products are absent and the set of equations (4) are:

$$\begin{aligned} Z_1 &= Y_1; \quad Z_2 = \mu_{22} Y_2; \\ Z_3 &= \mu_{32} Y_2 \\ Y_5 &= 1 - Z_1 - Z_2 - Z_3 \\ Y_3 &= Y_4 = 0 \end{aligned} \quad (5)$$

By considering a complete combustion of the hydrocarbon, the set of the balance equations for the case of rich mixture and lean mixture is respectively given by:

$$\left. \begin{aligned} Y_1 = 0; \quad Y_2 &= \frac{\left(\frac{\mu_{13}}{\mu_{14}}\right) z_2 + \left(\frac{\mu_{14}}{\mu_{34}}\right) z_3 - z_1}{\left(\frac{\mu_{13}\mu_{22}}{\mu_{23}}\right) + \left(\frac{\mu_{33}\mu_{14}}{\mu_{34}}\right)} \\ Y_3 &= \frac{z_2 - \mu_{22}Y_2}{\mu_{23}}; \quad Y_4 = \frac{z_3 - \mu_{32}Y_2}{\mu_{34}} \end{aligned} \right\} \quad (6)$$

And :

$$\left. \begin{aligned} Y_1 &= z_1 - \frac{\mu_{13}}{\mu_{23}} z_2 - \frac{\mu_{14}}{\mu_{34}} z_3; \quad Y_2 = 0 \\ Y_3 &= \frac{z_2}{\mu_{23}}; \quad Y_4 = \frac{z_3}{\mu_{34}} \end{aligned} \right\} \quad (7)$$

In the present work, the mixture fraction is defined as:

$$\xi = \frac{(Y_{N_2}^{\max} - Y_{N_2})}{(Y_{N_2}^{\max} - Y_{N_2}^{\min})} \quad (8)$$

Where  $Y_{N_2}$  is the mass fraction of nitrogen and the superscripts max and min correspond to pure air and fuel respectively.

It is worth noticing that, in the present situation, by considering methane-air combustion, the definition of the mixture fraction becomes: [23]

$$\xi = \frac{1 - Y_{N_2}}{Y_{N_2}^{\max}} \quad (9)$$

$Y_{N_2}^{\max} = Y_{N_2}^{air}$ , the mass fraction of nitrogen in air.

#### 4. Physical Analysis

We will report the analysis done by Veynante and Vervich [28] in order to derive the model predicting the occurrence of counter gradient turbulent diffusion. The flow field is assumed to be statistically one dimensional and only the turbulent transport in the propagation direction  $\overline{u''}c''$  will be described.

Following Bidaux and Bray [1994] (unpublished work already presented in the BML model context), turbulent fluxes of the progress variable  $c$ ,

$\overline{u''}c''$ , are directly connected to the surface -averaged fluctuating velocity,  $\langle u'' \rangle_s$ . Thus, a model for  $\overline{u''}c''$

may be deduced from a model for  $\langle u'' \rangle_s$  involving the conditional unburnt and burnt gases mean velocities:

$$\langle u'' \rangle_s = \langle u_i \rangle_s - \tilde{u}_i = (c^* - \tilde{c})(\overline{u_i^b} - \overline{u_i^u}) \quad (10)$$

This analysis is based on the two limiting cases which are: low turbulence level and high turbulence level.

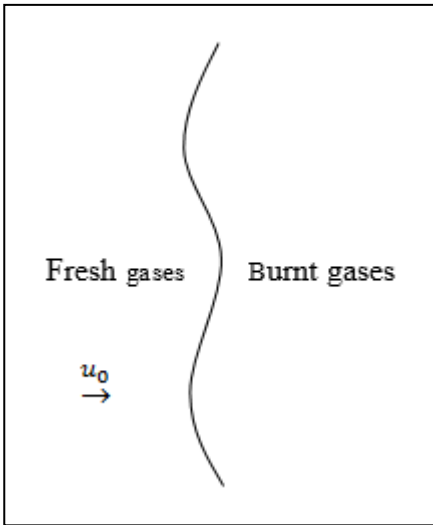


Fig.2 Low turbulence level

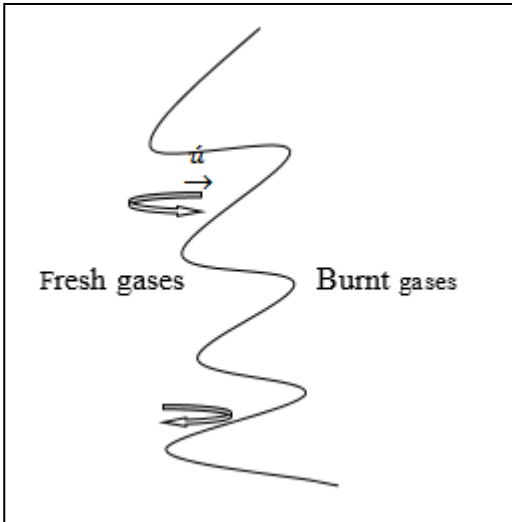


Fig.3 High turbulence level

In low turbulence level (Figure 2), the flame front remains smooth and the velocity jump between fresh and burnt gases,  $\overline{u}_i^b - \overline{u}_i^u$ , is determined by thermal expansion and its value is close to the one obtained in a plane laminar flame:

$$\overline{u}_i^b - \overline{u}_i^u \approx \tau S_L \quad (11)$$

And the equation (10) becomes :

$$\langle u'' \rangle_s = (c^* - \tilde{c}) \tau S_L \quad (12)$$

In high turbulence level (Figure 3), the flame front motions are assumed to be dominated by the turbulence properties taken upstream of the flame due to the strong viscous dissipation of turbulent eddies in the hot burnt gases.

At the leading edge of the turbulent flame (near  $\tilde{c} = 0$ ), the flame front is convected towards the fresh gases, with a mean velocity estimated by  $-u'$  (rms velocity in fresh gases) then

$$\overline{u}_i^b - \overline{u}_i^u = -u' \quad (13)$$

At the trailing edge of the flame brush ( $\tilde{c} \approx 1$ ), the flame front is convected by turbulent motions towards the burnt gases with a mean speed estimated by  $+u'$ .

$$\overline{u}_i^b - \overline{u}_i^u = +u' \quad (14)$$

Leading to the simple linear model:

$$\langle u'' \rangle_s = -2(c^* - \tilde{c})\alpha u' \quad (15)$$

Where  $\alpha$  is an efficiency function, similar to the ITNFS model proposed by Meneveau and Poinso [29].  $\alpha$  is expected to be of order unity for large turbulent length scales and the factor 2 has been introduced assuming  $c^* \approx 0.5$ .

Modeling  $\langle u'' \rangle_s$  as a sum of the two contributions lead to:

$$\langle u'' \rangle_s = (c^* - \tilde{c})(\tau S_L - 2\alpha u') \quad (16)$$

And the turbulent flux becomes:

$$\overline{u'' c''} = \tilde{c}(1 - \tilde{c})(\tau S_L - 2\alpha u') \quad (17)$$

This simple model was well verified in DNS by Veynante et al [21] and had also been recovered when applying a second order modeling to turbulent stagnating flames in the limit of small turbulence intensities by Bray et al [30].

This model presents the turbulent flux as a sum of two contributions acting in opposite directions, one induced by turbulent motions and the other by thermal

expansions. In case of high level turbulence, the turbulent transport is of gradient type and when the turbulence level is low, the thermal expansion due to the heat release dominates leading to a counter gradient diffusion.

We will now generalize this simple one dimensional model to our study. The transport equation of the progress variable is:

$$\frac{\partial \bar{\rho} \tilde{c}}{\partial t} + \frac{\partial \bar{\rho} \tilde{u}_i \tilde{c}}{\partial x_i} = \frac{\partial}{\partial x_i} \left( \bar{\rho} \frac{\mu}{\sigma} \frac{\partial \tilde{c}}{\partial x_i} - \overline{\rho u_i'' c''} \right) + \bar{\omega} \quad (18)$$

We assume that  $\alpha = 1$ , the equation (17) will be written as :

$$\overline{u'' c''} = \tilde{c}(1 - \tilde{c}) \tau S_L - 2u' \tilde{c}(1 - \tilde{c}) \quad (19)$$

The term  $2u' \tilde{c}(1 - \tilde{c})$  is modeled as the gradient

transport:  $-\frac{\mu_i}{\sigma} \frac{\partial \tilde{c}}{\partial x_i}$  and the term  $\tilde{c}(1 - \tilde{c}) \tau S_L$  in

two dimensions is modeled as:  $\tau S_L \langle n_f, n_i \rangle \frac{\partial \tilde{c}}{\partial x_i}$

Where  $\overline{n_f}$  is the unit vector normal to the flamelet front towards the burnt gases as shown in figure 4.

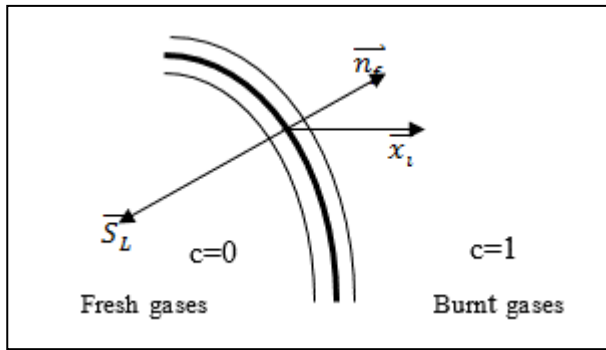


**Fig.4 Definition of unit vectors**

The normal vector to the flamelet may be written as :

$$\overline{n_f} = \frac{\overline{\nabla c}}{\|\overline{\nabla c}\|} \quad (20)$$

The equation (16) becomes:

$$\frac{\partial \bar{\rho} \tilde{c}}{\partial t} + \frac{\partial \bar{\rho} \tilde{u}_i \tilde{c}}{\partial x_i} = \frac{\partial}{\partial x_i} \left( \bar{\rho} \left( \frac{\mu}{\sigma} + \frac{\mu_t}{\sigma} \right) \frac{\partial \tilde{c}}{\partial x_i} - \bar{\rho} \tau S_L \langle n_f, n_i \rangle \frac{\partial \tilde{c}}{\partial x_i} \right) + \bar{\omega} \quad (21)$$

## 5. Mathematical Modeling

We use in this simulation the following assumptions:

- The flow is isenthalpic at low mach number.
- The Soret and the Dufour effects are neglected.
- The chemical reaction is a one step irreversible with a heat release parameter and a progress variable defined respectively as:

$$\tau = \frac{T_b - T_u}{T_u} \quad \text{And} \quad c = \frac{T - T_u}{T_b - T_u}$$

- The equation of state of the burnt and unburnt gases is that of an ideal gas:

$$\rho T = \rho_u T_u = \rho_b T_b = C^{te} \quad (22)$$

Which leads to:

$$\bar{\rho} = \frac{\rho_u}{1 + \tau \tilde{c}} \quad (23)$$

For an axisymmetric co-ordinate system (o,r,z), the equation of continuity, the momentum equations for the mean velocity components  $\tilde{u}$  and  $\tilde{w}$  and the equation for the mass-weighted Favre averaged progress variable  $\tilde{c}$  are given by :

$$\frac{1}{r} \frac{\partial}{\partial r} (r \bar{\rho} \tilde{u}) + \frac{\partial}{\partial z} (\bar{\rho} \tilde{w}) = 0 \quad (24)$$

$$\frac{1}{r} \frac{\partial r \bar{\rho} \tilde{u}_j \tilde{u}}{\partial x_j} = -\frac{1}{r} \frac{\partial r}{\partial x_j} (\overline{\rho u_j'' u''} - \bar{\tau}_{j1}) + \frac{\overline{\rho w''^2} - \bar{\tau}_{22}}{r} - \frac{\partial \bar{p}}{\partial r} \quad (25)$$

$$\frac{1}{r} \frac{\partial r \bar{\rho} \tilde{u}_j \tilde{w}}{\partial x_j} = -\frac{1}{r} \frac{\partial r}{\partial x_j} (\overline{\rho u_j'' w''} - \bar{\tau}_{j3}) + \frac{\overline{\rho w''^2} - \bar{\tau}_{22}}{r} - \frac{\partial \bar{p}}{\partial z} \quad (26)$$

$$\frac{1}{r} \frac{\partial r \bar{\rho} \tilde{u}_j \tilde{c}}{\partial x_j} = -\frac{1}{r} \frac{\partial}{\partial x_j} (r \overline{\rho u_j'' c''}) + \frac{1}{r} \frac{\partial}{\partial x_j} \left( r \frac{\mu}{S_c} \frac{\partial \tilde{c}}{\partial x_j} \right) + \bar{\omega} \quad (27)$$

$\tau_{ij}$  represent the viscous stresses and  $\overline{\rho u'' w''}$  are the Reynolds stresses.

$\bar{\omega}$  is the mean chemical production rate.

$\overline{\rho u_j'' c''}$  are the turbulent fluxes of the scalar  $c$ ,  $\mu$  is the molecular viscosity and  $S_c$  is the Schmidt number taken equal to 0.7.

### 5.1 Reynolds stress modeling

The balance equation for  $\overline{\rho u_i'' u_j''}$  for a variable density flow given by Launder et al. [31] is:

$$\frac{1}{r} \frac{\partial r \tilde{u}_k \overline{\rho u_i'' u_j''}}{\partial x_k} = \frac{1}{r} \frac{\partial}{\partial x_k} \left( r C_s \frac{k}{\varepsilon} \overline{\rho u_k'' u_m''} \frac{\partial \overline{\rho u_i'' u_j''}}{\partial x_m} / \bar{\rho} \right) + \frac{1}{r} \frac{\partial}{\partial x_k} \left( r \mu \frac{\partial \overline{\rho u_i'' u_j''}}{\partial x_j} / \bar{\rho} \right) + P_{ij} + G_{ij} + \Phi_{ij} - \frac{2}{3} \bar{\rho} \varepsilon \delta_{ij} \quad (28)$$

Where : The production due to the mean velocity gradient  $P_{ij}$  is:

$$P_{ij} = -\overline{\rho u_i'' u_k''} \frac{\partial \tilde{u}_j}{\partial x_k} - \overline{\rho u_j'' u_k''} \frac{\partial \tilde{u}_i}{\partial x_k} \quad (29)$$

The interaction between the velocity fluctuations and the mean pressure gradient  $G_{ij}$  is:

$$G_{ij} = -\frac{\tau}{\rho_u} \left( \overline{\rho u_i'' c''} \frac{\partial \bar{p}}{\partial x_j} + \overline{\rho u_j'' c''} \frac{\partial \bar{p}}{\partial x_i} \right) \quad (30)$$

The pressure strain correlation  $\Phi_{ij}$  is :

$$\Phi_{ij} = -C_1 \frac{\tilde{\varepsilon}}{k} \left( \overline{\rho u_i'' u_j''} - \frac{2}{3} \delta_{ij} \bar{\rho} k \right) - C_2 \left( P_{ij} - \frac{1}{3} P_{kk} \delta_{ij} \right) - C_3 \left( G_{ij} - \frac{1}{3} G_{kk} \delta_{ij} \right) \quad (31)$$

The values of the constants  $C_1$ ,  $C_2$ ,  $C_3$  and  $C_s$  are taken equal to 1.8, 0.6, 0.55 and 0.22 respectively.

### 5.2 Combustion modeling

We use the LW-P model for partially premixed combustion developed by Robin et al [23].

This model is based on the LW model developed by Libby and Williams [24]. The LW model is based on two independent thermo dynamical quantities: the fuel mass fraction  $Y_f$  and the mixture fraction  $\xi$ . All species are related to these two scalars.

The balance equation for the mean fuel mass fraction  $Y_f$  is written as:

$$\frac{\partial \bar{\rho} \tilde{Y}_f}{\partial t} + \frac{1}{r} \frac{\partial}{\partial r} (r \bar{\rho} \tilde{u} \tilde{Y}_f) + \frac{\partial \bar{\rho} \tilde{w} \tilde{Y}_f}{\partial z} = \frac{1}{r} \frac{\partial}{\partial r} \left[ r \left( \frac{\mu}{S_c} \frac{\partial \tilde{Y}_f}{\partial r} - \overline{\rho u'' Y_f''} \right) \right] + \frac{\partial}{\partial z} \left( \frac{\mu}{S_c} \frac{\partial \tilde{Y}_f}{\partial z} - \overline{\rho w'' Y_f''} \right) + \bar{\omega} \quad (32)$$

The turbulent fluxes  $\overline{\rho u'' Y_f''}$  and  $\overline{\rho w'' Y_f''}$  are closed by the new model described in section 4 as:

$$\overline{\rho u'' Y_f''} = -\frac{\mu_i}{S_c} \frac{\partial \tilde{Y}_f}{\partial r} + \tau S_L \langle n_f, n_r \rangle \frac{\partial \tilde{Y}_f}{\partial r} \quad (33)$$

$$\text{and } \overline{\rho w'' Y_f''} = -\frac{\mu_t}{S_c} \frac{\partial \tilde{Y}_f}{\partial z} + \tau S_L \langle n_f, n_z \rangle \frac{\partial \tilde{Y}_f}{\partial z} \quad (34)$$

The fuel consumption rate  $\bar{w}$  appearing as a source term in the transport equation (32) for the mean value of the fuel mass fraction is a function of  $\xi$  and  $Y_f$  and it is written as:

$$\bar{w} = \rho(\xi, Y_f) B(\xi) (Y_f - Y_f^{\min}) \exp\left(\frac{-T_a}{T(\xi, Y_f)}\right) \quad (35)$$

Where

$Y_f^{\min}$  is the minimum value of  $Y_f$ .

$$Y_f^{\min} = 0 \text{ for lean mixtures and } Y_f^{\min} = \frac{\xi - \xi_{st}}{1 - \xi_{st}} \text{ for}$$

rich mixtures.

$B(\xi)$  the pre-exponential factor is assumed to be a

function of the mixture fraction.

The balance equation for the mixture fraction and its variance are written as:

$$\frac{\partial \bar{\rho} \tilde{\xi}}{\partial t} + \frac{1}{r} \frac{\partial}{\partial r} (r \bar{\rho} \tilde{u} \tilde{\xi}) + \frac{\partial \bar{\rho} \tilde{w} \tilde{\xi}}{\partial z} = \frac{1}{r} \frac{\partial}{\partial r} \left[ r \left( \frac{\mu}{S_c} + \frac{\mu_t}{\sigma_f} \right) \frac{\partial \tilde{\xi}}{\partial r} \right] + \frac{\partial}{\partial z} \left[ \left( \frac{\mu}{S_c} + \frac{\mu_t}{\sigma_f} \right) \frac{\partial \tilde{\xi}}{\partial z} \right] \quad (36)$$

$$\frac{\partial \bar{\rho} \xi^2}{\partial t} + \frac{1}{r} \frac{\partial}{\partial r} (r \bar{\rho} \tilde{u} \xi^2) + \frac{\partial \bar{\rho} \tilde{w} \xi^2}{\partial z} = \frac{1}{r} \frac{\partial}{\partial r} \left[ r \left( \frac{\mu}{S_c} + \frac{\mu_t}{\sigma_f} \right) \frac{\partial \xi^2}{\partial r} \right] + \frac{\partial}{\partial z} \left[ \left( \frac{\mu}{S_c} + \frac{\mu_t}{\sigma_f} \right) \frac{\partial \xi^2}{\partial z} \right] + 2 \frac{\mu_t}{\sigma_f} \left[ \left( \frac{\partial \tilde{\xi}}{\partial r} \right)^2 + \left( \frac{\partial \tilde{\xi}}{\partial z} \right)^2 \right] \quad (37)$$

## 6. Numerical Simulation

We will be referred to the conditions of the experimental study of D. Escudié et al. [10,11].

### 6.1 Computational geometry

The computational domain used for the flame impinging onto the wall simulation shown in figure 5 extends to 330 mm (10 times the radius of the burner) in the radial direction.

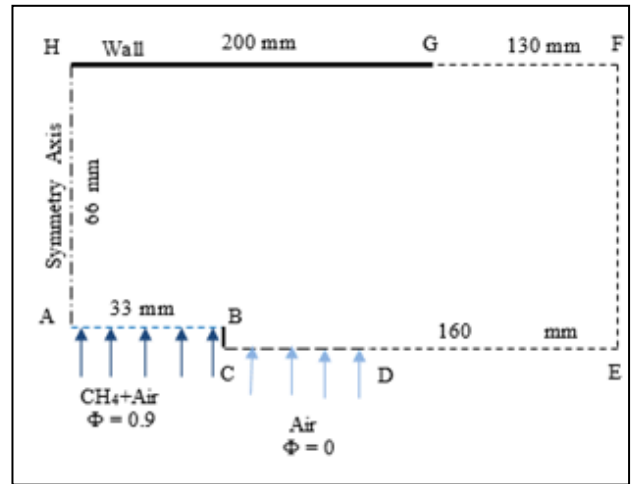


Fig.5 Computational domain

### 6.2 Boundary conditions

The following boundary conditions are prescribed:

At the burner exit AB, the velocity  $W$ , the turbulence kinetic energy and the integral length scale are fixed respectively at 4 m/s, 0.135 m<sup>2</sup>/s<sup>2</sup>, 1 mm [16].

At the inlet of dilution CD, the following conditions are based on a non reacting flow simulation; a fourth degree polynomial is fitted:

$$u(r) = 610 r^4 - 340 r^3 + 62 r^2 - 5 r + 0.068$$

$$w(r) = 1400 r^4 - 980 r^3 + 230 r^2 - 19 r + 0.63$$

Along the solid walls HG and BC, standard wall functions along and the fluxes are set to zero for all scalars.

On the free boundaries DE, EF and FG, the radial derivatives of all variables are set to zero.



On the centerline HA, symmetry conditions are imposed so that the radial component of the velocity and the radial derivatives of all the remaining variables are set to zero.

### 7. Results and Discussions

The model described in the previous sections has been implemented in the computational fluid dynamics (CFD) code developed by EDF: code saturne [32].

Code saturne is a parallel general purpose three dimensional low mach number CFD code based on a finite volume method. A computational domain representing half of the physical space of size 66 mm in the axial direction,  $z$ , and 330 mm in the radial direction,  $r$ , is used with a refined grid near the fuel exit and the centerline of the burner. The smallest cell size is  $0.5 \times 0.1$  (in mm) and it is found in the present study that the grid size of 27575 cells for the geometry ensures a grid independent solution.

Non reacting case:

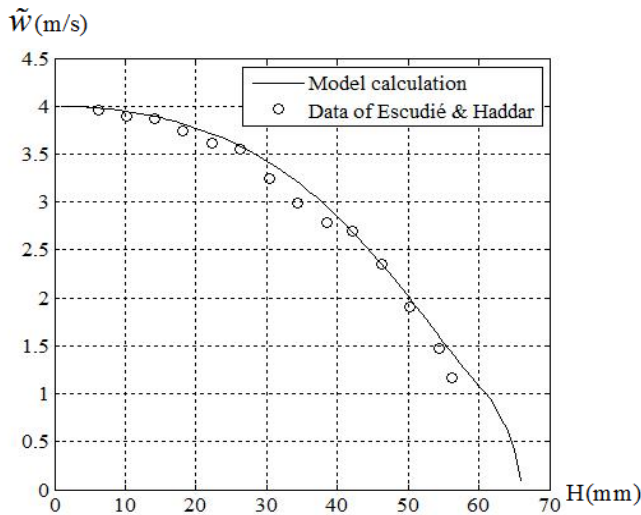


**Fig. 6** Calculated mean axial velocity profile along the centerline of the burner

The non reacting flow case was simulated first to assess the turbulence model and the flow boundary conditions used.

Figure 6 shows a good agreement between the predicted mean axial velocity at the centerline of the burner against the experimental data of Escudié and Haddar [4, 5].

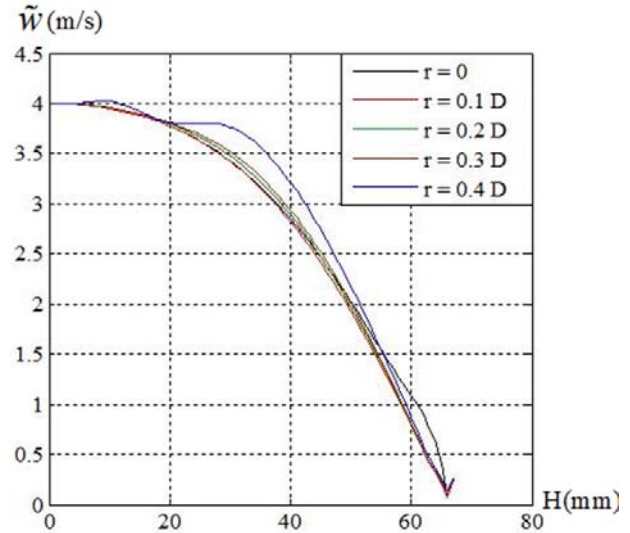


**Fig. 7.** Calculated mean axial velocity profile at different radial positions

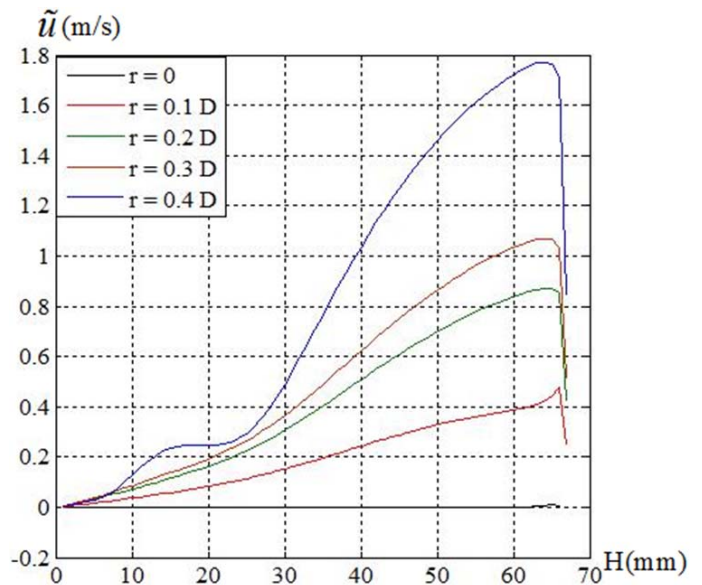


**Fig. 8.** Calculated mean radial velocity profile different radial positions

Figure 7 and figure 8 display the evolution of the mean axial velocity and the mean radial velocity at different radial positions. It is shown that the mean axial velocity decreases from its maximum of 4 m/s value at the exit of the burner to its minimum value 0

m/s at the stagnating plate. The profile of the mean axial velocity is independent from the radial position.

Concerning the mean radial velocity, its profile changes with the same shape when increasing in the radial position. It reaches its maximum value of 1.76 m/s at the periphery of the nozzle exit at the stagnating plate due to the parietal flow.

The simulation of the non reacting flow is done in order to assess the turbulence model and the flow boundary conditions used which allows the generation of a guest solution field for simulating the reactive flow.

Reacting case:

Initially, the flow was solved for a non reacting case with complete species transport. Once a converged solution is obtained for a non reacting case, a flame is initiated at the centerline of the jet near the wall by introducing a high temperature patch for the first fifty iterations in the computational domain. Although, different simulations were done and after analyzing them, they led to the same flame shape and location at the end of the converged solution.

The solution is deemed to be converged when the scaled residuals of mass, momentum, energy and various combustion species had dropped to  $10^{-5}$  and there was no appreciable change in the respective residuals further.

To validate the numerical model, our present solution is compared with the experimental data of Escudié and Haddar [4, 5] and the numerical simulation of Lahjaily et al [10].

Figure 9 shows the predicted results of the mean axial velocity along the centerline axis of the burner compared to the measured values by Escudié and Haddar and the computational results of Lahjaily et al.

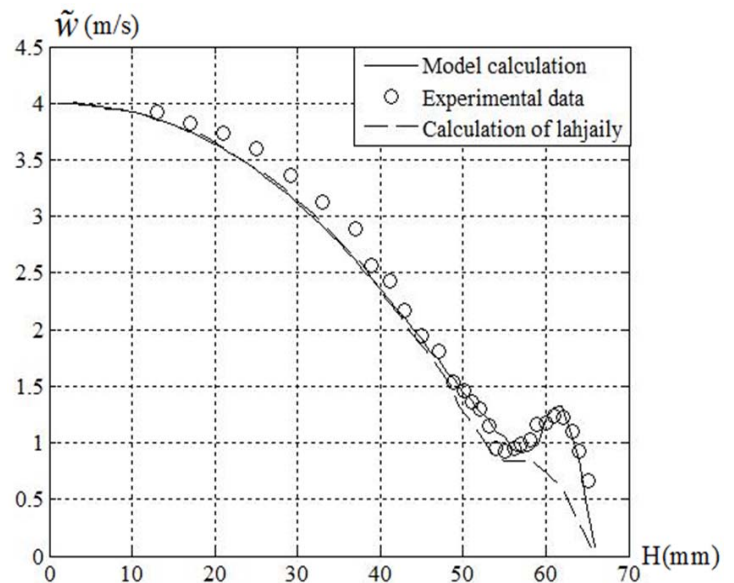
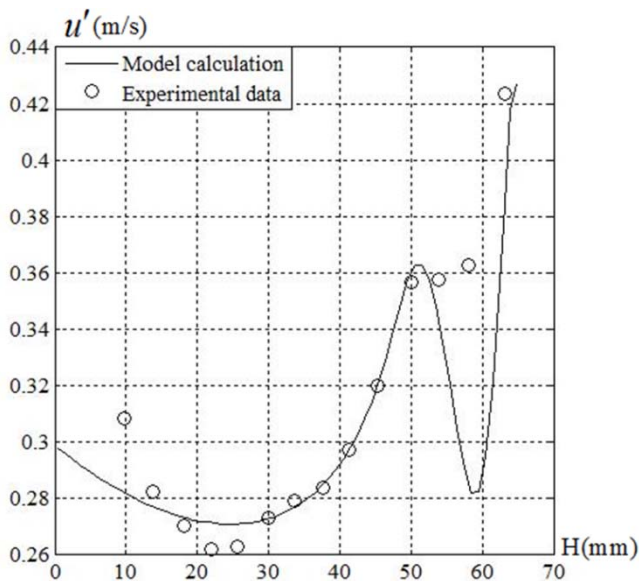


Fig. 9. Evolution of the mean axial velocity along the centerline axis

A qualitatively and a quantitatively good agreement is obtained. The level of the jump of the velocity behind the flame brush is well predicted by our model. It is shown that the calculations given by the model of Lahjaily where the turbulent fluxes is modeled as a gradient type has really underestimated the velocity jump across the flame. The agreement between our results and the experimental data can be explained by the fact that flame generated disturbances is produced by velocity gradients induced by the pressure drop (pressure decreases from unburned to burned region) across the combustion zone associated with the density decrease of the gases upon passage through the flame front is found to decrease flame wrinkling and turbulent flame speed and will promote counter gradient turbulent transport.

Figure 10 shows the evolution of the rms radial velocity fluctuations. The agreement between the predicted and the measured values is quite good. Due to heat release, gas density decreases within the instantaneous flame front, and the variation in density affect the flow velocity by virtue of mass conservation

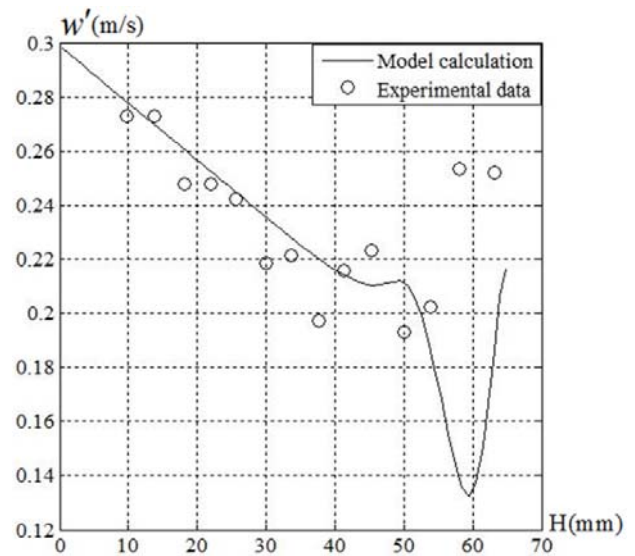
which induce some changes in the magnitude of some terms in the governing equations.



**Fig. 10. Evolution of the velocity rms radial fluctuation along the centerline axis**

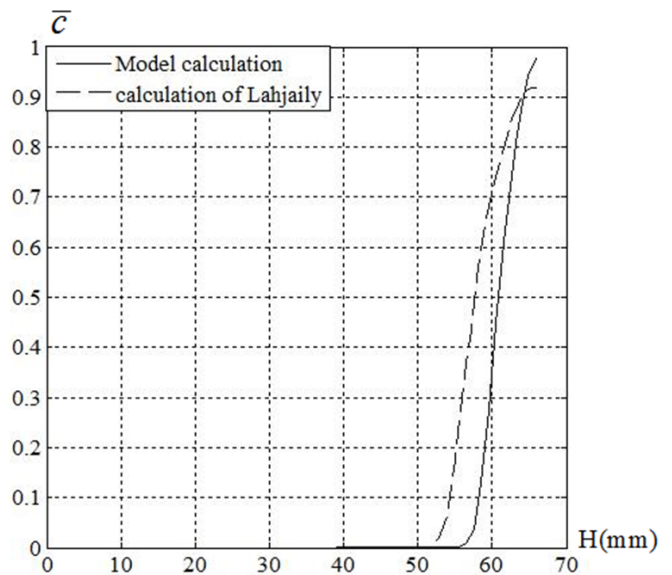
The calculations done by the model show spreading of the profile in front of the flame compared to the experimental data.

Figure 11 shows a quantitative disagreement of the evolution of the rms axial fluctuations. The differences between predictions and measurements are higher at smaller distances from the wall. It should be stressed that the predicted fluctuating axial velocity does not exceed the measured values near the wall in the stagnation flow region which is the stress limiter. Although, the present model predict qualitatively the production of turbulence through the flame brush but it fail to predict the values of these fluctuations. The reason for these discrepancies is due to the effect of the strong pressure gradient across the flame brush and the fact that the pressure fluctuations were neglected during this simulation.



**Fig. 11. Evolution of the velocity rms axial fluctuation along the centerline axis**

Figure 12 shows the evolution of the mean progress variable along the centerline of the jet. The profile is correctly predicted by the present model. A light difference is in the thickness of the flame brush. The present model predict a flame brush thinner than the model of Lahjaily.



**Fig. 12. Evolution of the mean progress variable along the centerline axis**

The turbulent flame brush is defined as a relatively thick zone consisting of thin reaction zones that separate unburned reactants from burned products and that are transported by the turbulent eddies randomly. The flamelet regime in which the chemical reactions controlling heat release are confined to thin, highly wrinkled, convoluted, and strained interfaces separating unburned reactants from burned products is associated mainly with large scale, weak and moderate turbulence.

The flame brush defined as the region where  $0.1 < \overline{C} < 0.9$ , is about 6 mm thick in our model but it is more than 10 mm in the predictions of Lahjaily et al. which was away from the experimental observations.



**Fig. 13. Field of the mean flame brush**

Figure 13 shows the field of the mean flame brush which shows a stabilized stretched turbulent flame brush closed to the wall detached from the burner as observed in the experiment. The divergent flow generated by flow impingement on a stagnation plate allows the flame to position itself at a short distance upstream on the stagnation point.

The thickness of the turbulent brush is controlled by the random motion of the front around its mean position under the influence of turbulent eddies.

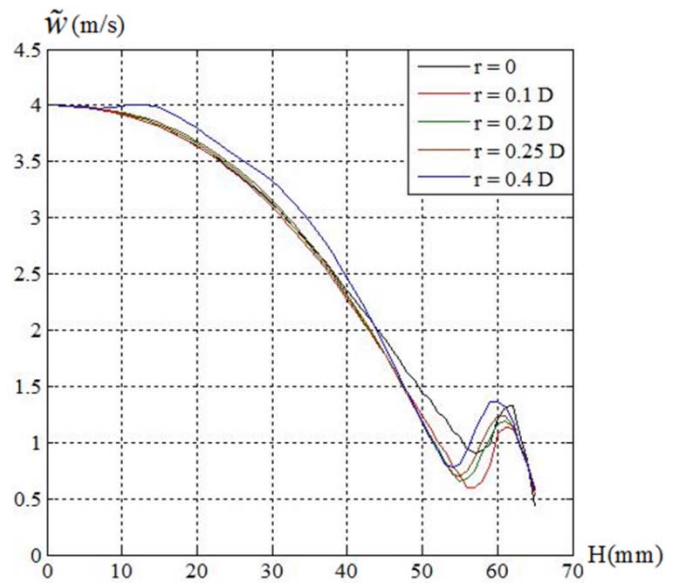


**Fig. 14. Evolution of the axial profile of the mean axial velocity at different radial positions**

Figure 14 shows that the axial profiles of the Favre mean axial velocity at different radial positions are similar. The velocity decrease from 4 m/s at the exit of the burner to 0.9 m/s in front of the flame brush and jump to its maximum value across the flame and reach its minimum value of zero near the wall. The superimposed profiles for the different radial positions show that we still in the case of planar flames.

Figure 15 shows that the axial profile of the Favre mean radial velocity increase linearly in the potential core and suddenly it increases strongly behind the flame brush. It seems varying linearly with the radius. It is significantly higher near the wall due to gas expansion and reaches its maximum value far from the centerline.

Our comparison was confined to the mean axial velocities at the centerline of the burner but since the data on radial gradient of the mean radial velocity are difficult to obtain and are of questionable accuracy, figure 15 shows an excellent representation of the

evolution of the gradient of the mean radial velocity in the considered experiment.

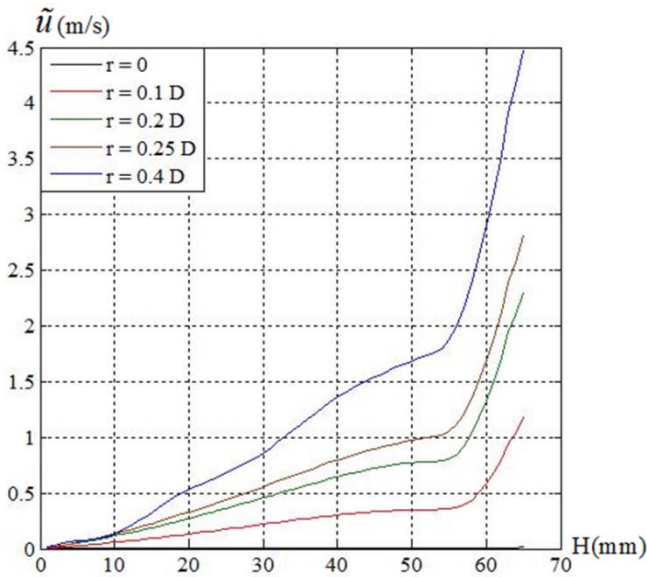


Fig. 15. Evolution of the axial profile of the mean radial velocity at different radial positions

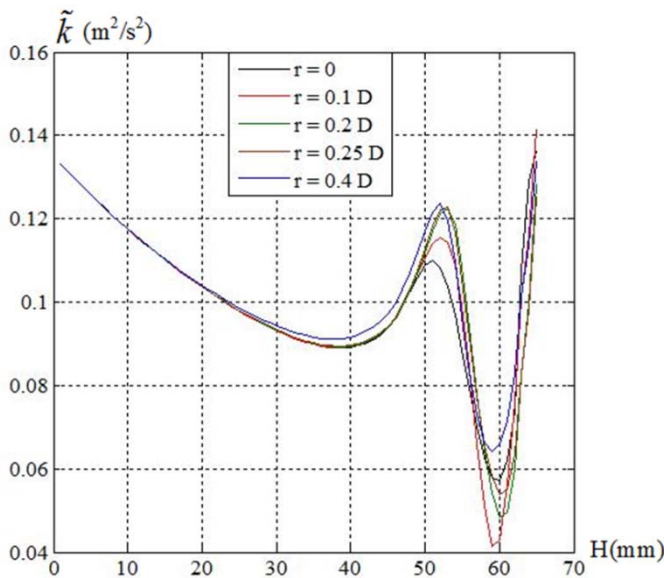


Fig. 16. Evolution of the axial profile of the mean turbulent kinetic energy at different radial positions

Figure 16 displays the evolution of the axial profile of the Favre mean turbulent kinetic energy at different radial positions. It is shown that the predictions results behind the flame brush are weak compared to the experiments in all kinds of flames impinging onto a wall which might be the effect of too weak turbulence mixing in the free shear layer predicted by the Rij- $\epsilon$  model. However, it might be expected that the gas expansion associated with heat release would result in pressure fluctuations significantly which call for a special attention. It should be worth noticing that this deficiency seems to have no effect on the predicted mean velocities.

Figure 17 displays the evolution of the axial profile of the Favre mean temperature at different radial positions. It is shown that the flame is thin and plane and the thickness of the flame increases when the radius increases due to the stretch of the flame and its curvature which correspond really to the experimental observations.

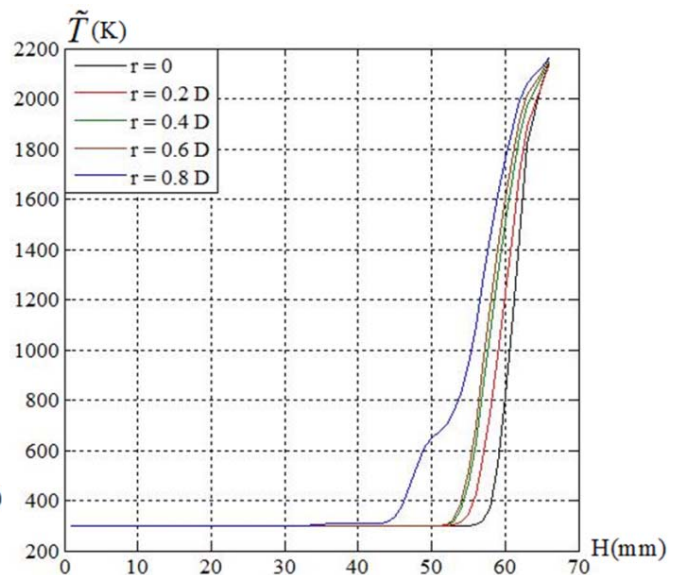


Fig. 17. Evolution of the axial profile of the mean temperature at different radial positions

## 8. Conclusion

An algebraic model closure of turbulent scalar fluxes is proposed to take into account the flame generated disturbances which are produced by velocity gradients induced by the pressure drop across the combustion zone associated with the density decrease of the gases upon passage through the flame front.

A numerical simulation which corresponds to the experimental conditions of the experiment of Escudié and Haddar was presented in order to validate the model against a turbulent premixed flame impinging onto a wall where experimental investigations of counter gradient scalar transport were performed and associated with the flamelet regime of premixed turbulent combustion.

The comparison of the results with the measurements were showing remarkable consistency and indicates that the model is a valid approach for predicting partially turbulent premixed flames stabilized in a stagnation flow.

The evolution of all the parameters is done in the full domain not only at the centerline which is usually done.

## References

- [1] M. Day and J. Bell, "Simulation of Turbulent Premixed Flames", *Journal of physics: conference series*, Vol. 46, pp. 43-47, (2006).
- [2] A Y. Klimenko and R. W. Bilger, "Conditional moment closure for turbulent combustion", *Progress in Energy and Combustion Science*, Vol. 25, pp. 595-687, (1999).
- [3] A. Mura and M. Champion, "Relevance of the Bray number in the small scale modeling of turbulent premixed flames", *Combustion and Flame*, Vol. 156, 729-733, (2009).
- [4] J.A. Van Oijen, R. J. M. Bastiaans, G. R. A. Groot and L. P. H. De Goey, "Direct numerical simulations of premixed turbulent flames with reduced chemistry; validation and flamelet analysis", *Flow, Turbulence and Combustion*, Vol. 75, pp. 67-84, (2005).
- [5] N. Peters, "Turbulent combustion", Cambridge University Press, Cambridge (2000)
- [6] R. W. Bilger, S. B. Pope, K. N. C. Bray and J. F. Driscoll, "Paradigms in turbulent combustion research", *Proceedings of the Combustion Institute*, Vol. 30, pp. 21-42 (2005).
- [7] T. Poinso and D. Veynante, "Theoretical and Numerical Combustion", Edwards, Philadelphia, PA, USA, 2nd Edition, (2005).
- [8] A. N. Lipatnikov, "Fundamentals of Premixed Turbulent combustion", CRC Press, (2012).
- [9] P. Cho, C. K. Law, J. R. Hertzberg and R. K. Cheng, "Velocity and scalar fields of turbulent premixed flames in stagnating flow", *Twenty second symposium (international) on combustion/ The combustion institute*, pp. 739-745, (1988).
- [10] D. Escudié and E. Haddar, "Experimental study of a premixed turbulent stagnating flame", *Combustion and Flame*, Vol. 95, pp. 433-435, (1993).
- [11] D. Escudié, E. Haddar and M. Brun, "Influence of strain rate on a premixed turbulent flame stabilized in a stagnating flow", *Experiments in fluids*, Vol. 27, pp. 533-541, (1999).
- [12] S.C. Li, P. A. Libby and F. A. Williams, "Experimental investigation of a premixed flame in an impinging turbulent stream", *Twenty-fifth symposium (International) on combustion/ The combustion institute*, pp. 1207-1214, (1994).
- [13] R.K. Cheng and I.G. Shepherd, "The influence of burner geometry on premixed turbulent flame propagation", *Combustion and flame*, Vol. 85, pp. 7-26 (1991).
- [14] W.D. Hsieh, S. S. Hou and T. H. Lin, "Methane flames in a jet impinging onto a wall", *Proceedings of the Combustion Institute*, Vol. 30, pp. 267-275 (2005).
- [15] K.N.C. Bray, M. Champion and P.A. Libby, "Premixed flames in stagnating turbulence, Part I –The general formulation for counter flowing streams and gradient models for turbulent transport", *Combustion and Flame*, Vol. 84, pp. 391-410 (1991).
- [16] H. Lahjaily, D. Karmed and M. Champion, "Introduction of dilution in the BML model: Application to a stagnating turbulent flame", *Combust. Sci. Technol.*, Vol. 135, pp. 153-173 (1998).
- [17] D. Karmed, H. Lahjaily and M. Champion, "Influence of the turbulent Damkohler number on the structure of premixed flames in a stagnation flow", *Combust. Sci. Technol.*, Vol. 113, pp. 351-365 (1996).

- [18] P. Clavin and F. A. Williams, "Theory of premixed flame propagation in large scale turbulence", *Journal of fluid mechanics*, Vol. 90(3), pp. 589-604 (1979).
- [19] P.A. Libby and K.N.C. Bray, "Countergradient diffusion in premixed turbulent flames", *AIAA journal*, Vol. 19(2), pp. 205 (1981).
- [20] P.A. Kalt, Y.C. Chen and R.W. Bilger, "Experimental investigation of turbulent scalar flux in premixed stagnation type flames", *Combustion and Flame*, pp. 401-415, 2002.
- [21] D. Veynante, A. Trouvé, K.N.C. Bray and T. Mantel, "Gradient and Counter-Gradient Scalar Transport in Turbulent Premixed Flames", *Journal of Fluid Mechanics*, Vol. 332, pp. 263-293, (1997).
- [22] K.N.C. Bray, M. Champion and P. A. Libby, "Thermochemistry revisited flows", *Combust. Sci. Technol.*, Vol. 174(7), pp. 167-174, (2002).
- [23] V. Robin, A. Mura, M. Champion and P. Plion, "A multi Dirac presumed PDF model for turbulent reactive flows with variable equivalence ratio", *Combust. Sci. Technol.*, Vol. 178(10-11), pp. 1843-1870 (2006).
- [24] P.A. Libby and F.A. Williams, "A presumed Pdf analysis of partially premixed turbulent combustion", *Combust. Sci. Technol.*, Vol. 161, pp. 351-390, (2000).
- [25] V.A. Sabel'nikov and A.N. Lipatnikov, "A simple model for evaluating conditioned velocities in premixed turbulent flames", *Combust. Sci. Technol*, Vol. 183, pp. 588-613 (2011).
- [26] G. Ribert, M. Champion and P. Plion, "Modeling nonadiabatic turbulent premixed reactive flows including tabulated chemistry", *Combustion and Flame*, Vol. 141, pp. 271-280, (2005).
- [27] V. Robin, A. Mura, M. Champion and A. Boukhalfa, "Experimental and numerical analysis of stratified turbulent V-shaped flames", *Combustion and flame*, Vol. 153, pp. 288-315, (2008).
- [28] D. Veynante and L. Vervich, "Turbulent combustion modeling", *Progress in Energy and Combustion Science*, Vol. 28, pp. 193-266, (2002).
- [29] C. Meneveau and T. Poinso, "Stretching and Quenching of Flamelets in Premixed Turbulent Combustion", *Combustion and Flame*, Vol. 86, pp. 311-332, (1991).
- [30] K.N.C. Bray, M. Champion and P.A. Libby, "Premixed Flames in Stagnating Turbulence, Part IV – A New Theory for the Reynolds Stresses and Reynolds Fluxes Applied to Impinging Flows", *Combustion and Flame*, Vol. 120, pp. 1-18, (2000).
- [31] B.E. Launder, G. J. Reece and W. Rodi, "Progress in the development of a Reynolds-stress turbulence closure", *J. Fluid. Mech*, Vol. 68, pp. 537-566, (1975).
- [32] F. Archambeau, N. Méchitoua and M. Sakiz, "Code Saturne: A finite volume code for turbulent flows", *Intl J. of Finite Volumes*, Vol. 1, pp. 1-62, (2004). M. Young, *The Technical Writer's Handbook*. Mill Valley, CA: University Science, 1989.